Nanotechnology 17 (2006) 2181–2186 doi:10.1088/0957-4484/17/9/017

Effect of surface states on carrier dynamics in InGaAsP/InP stressor quantum dots

J Riikonen[1], J Sormunen, H Koskenvaara, M Mattila, A Aierken, T Hakkarainen, M Sopanen and H Lipsanen

Optoelectronics Laboratory, Micronova, Helsinki University of Technology, PO Box 3500, FIN-02015 HUT, Finland

E-mail: juha.riikonen@tkk.fi

Received 23 December 2005
Published 31 March 2006
Online at stacks.iop.org/Nano/17/2181

Abstract
The carrier dynamics in strain-induced InGaAsP/InP quantum dots (QDs) is investigated by time-resolved photoluminescence and continuous-wave photoluminescence. The stressor QDs are fabricated by depositing self-assembled InAs islands (or stressor islands) on top of a near-surface InGaAsP/InP quantum well (QW). The temporal behaviour of the QD photoluminescence transients are observed to exhibit a two-phase decay. Rate equation analyses reveal that by increasing the distance of the QW from the surface the surface capture time constant is increased considerably while the capture time constant of an electron from the QW to the QD is decreased.

1. Introduction

Stressor quantum dot or strain-induced quantum dot (SIQD) structure is an almost ideal system for fundamental investigations of quantum dots (QDs) [1–4]. These nearly-perfect QDs can be fabricated by utilizing self-assembled islands as stressors to induce a tensile strain which deforms the energy band structure locally, creating a lateral confinement potential [5]. The underlying near-surface quantum well (QW), in turn, provides a vertical confinement, and, as a result, a QD is formed in the QW. Besides the fundamental QD investigation, SIQDs also provide an excellent means to study the interplay between the islands and the QW in general. This is advantageous, since similar effects have an important role in determining, for example, the characteristics of buried QD structures utilizing strained layers and the transport properties of a two-dimensional electron gas in the vicinity of QDs [6, 7].

Figure 1(a) shows the structure of the strain-induced QD sample. A schematic diagram of the deformation of the conduction and valence bands along with a typical SIQD photoluminescence (PL) spectrum are shown in (b) and (c), respectively. The QD ground state is labelled with QD0 and the excited states with QD1 and QD2. Figure 1(d) shows the calculated effect of the QW-to-surface distance d on the confinement potential.

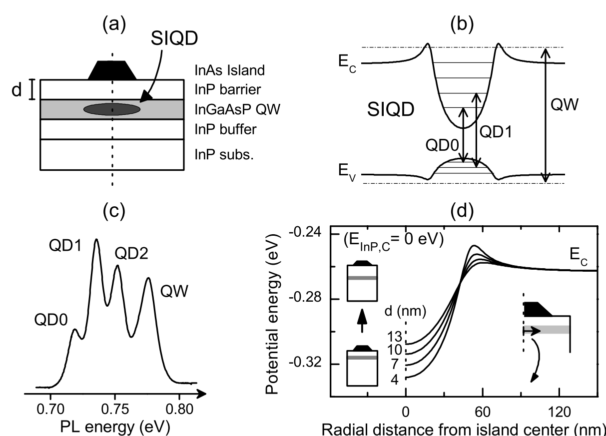

Figure 1. (a) Schematic diagram of the SIQD structure, (b) the in-plane confinement potential of an SIQD, (c) typical PL spectrum, and (d) the effect of the QW-to-surface distance d on the confinement potential. (The base diameter of the island is 110 nm.)

Previously, InGaAs/GaAs SIQDs utilizing InP stressors have proved to be of high quality [2, 4]. In fact, InP is

[1] Author to whom any correspondence should be addressed.

© 2006 IOP Publishing Ltd Printed in the UK

quite a suitable stressor material for the GaAs-based system, since (i) the lattice mismatch of InP/GaAs (3.8%) allows coherent islands up to about 120 nm in diameter and (ii) InP passivates the GaAs surface, thus reducing surface recombination [5, 8–10]. Wang *et al* [10] reported that InGaAs/GaAs SIQDs can also be fabricated by using GaSb islands. As they pointed out, however, the fact that GaSb has a lower band gap (0.81 eV at $T = 10$ K) compared to that of InP (1.42 eV) will certainly enhance the surface recombination. Moreover, due to the large lattice mismatch of GaSb/GaAs (7.8%) the maximum diameter of coherent GaSb islands is only 36 nm [10]. As a consequence, the achieved depth of the confinement potential is quite small. Surface recombination is typically considered to be detrimental to the optical and electrical characteristics, especially in low-dimensional structures. In a non-saturable absorber utilizing a single, near-surface QW [13], however, surface recombination (capture) is used to reduce the carrier lifetime.

Recently, a highly tunable InGaAsP/InP SIQD structure utilizing InAs islands has also been reported [11, 12]. The lattice mismatch of the InAs/InP stressors (3.2%) is roughly the same as in the case of the InP/GaAs stressor system. Interestingly, despite the fact that InAs is also a low band gap material (0.42 eV), the SIQDs using InAs stressors have shown good optical characteristics [11, 12], contrary to the GaSb stressor system [10].

In this work, the carrier dynamics of InGaAsP/InP strain-induced QDs is studied. Time-resolved PL (TRPL) and continuous-wave PL (cw-PL) are used to investigate the QD characteristics. Varying the QW-to-surface distance d from 4 to 13 nm is found to dramatically increase the carrier lifetime in the QDs. The rate equation model is applied to study the carrier dynamics.

2. Experimental details

The samples investigated in this study were fabricated by metalorganic vapour phase epitaxy (MOVPE) on InP(001) substrates. Details of the SIQD growth process are given elsewhere [12, 14, 15]. The samples consisted of InAs stressor-islands deposited on a 10 nm thick near-surface $In_{0.78}Ga_{0.22}As_{0.59}P_{0.41}$/InP QW. As determined by atomic force microscopy (AFM), the island density is approximately 2×10^9 cm^{-2} and the typical base diameter and the height of the islands are 110 nm and 22 nm, respectively. A set of four samples with varying QW barrier thickness d was fabricated ($d = 4$, 7, 10 and 13 nm). For reference, near-surface QW samples without InAs and samples with a mere InAs wetting layer (no islands) were also fabricated.

The conduction band confinement potential was calculated using the ΔT finite element method (ΔT FEM) [1]. A cylindrical symmetry is assumed in the computation. The increasing strain in the QW along with decreasing d is seen to result in a deeper confinement potential and higher in-plane barriers around it (as shown in figure 1(d)). For clarity, in this paper, the potential barriers around the central minimum are referred to as in-plane barriers, and the InP barrier of the QW is referred to as the QW barrier. Barrier thickness refers always to d (i.e., the distance from the QW to the surface).

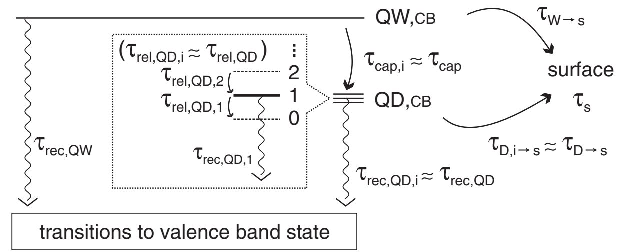

Figure 2. Simplified energy level and transition schematic diagram of the SIQD. Transitions involving QD1 are shown in more detail.

Low-temperature (10 K) time-resolved PL measurements were conducted in order to study the carrier dynamics. The TRPL measurements were performed by exciting the samples with 150 fs pulses at 800 nm from a mode-locked Ti:sapphire laser with a repetition rate of 76 MHz. The signal was detected by a Peltier-cooled (∼−30 °C) microchannel plate photomultiplier (Hamamatsu C2773) and time-correlated single photon counting electronics. The (long-wavelength) luminescence from the samples is out of the main spectral response range of the detector. However, the high PL intensity of the samples enabled the measurements at the cut-off region of the detector. Time-resolved PL curves in this work are corrected with the detector response. The temporal resolution of the system is approximately 30 ps. In the cw-PL a frequency-doubled Nd:YVO_4 laser operating at 532 nm was used for excitation. The signal was recorded using a 0.5 m monochromator with a liquid-nitrogen-cooled germanium detector while utilizing standard lock-in techniques.

3. Rate equation model

The temporal PL characteristics of InGaAs/GaAs strain-induced QDs utilizing InP stressors have been shown to be d-independent, meaning that the surface recombination is insignificant [9]. In that report, it was assumed that this behaviour is due to protective nature of InP (in the stressor islands). Carriers in the QW, on the other hand, were observed to experience increased tunnelling into surface states when the QW was closer to the surface. In a recent report, InGaAsP/InP SIQD PL was observed to be affected by surface recombination [16]. It was shown that the typical rate equation model including only the energy states of the QD [4] was not adequate. Moreover, a model including the QW and the surface related transitions was shown to agree with the temporal characteristics of the SIQD system [16]. Hence, the QW and the surface related transitions are included in the model used in this work also.

The background doping of the samples fabricated by the MOVPE reactor used in this work is typically p-type. Moreover, holes relax typically much more rapidly than electrons due to smaller level spacing. Therefore, the temporal behaviour of the PL peaks is governed by the electron populations, and holes can be excluded from the model.

Figure 2 shows a simplified schematic diagram of the energy structure and the transitions in an SIQD structure. After the excited electrons have relaxed to the QW ground state they are mainly recombined radiatively (with a time

constant $\tau_{rec,QW}$) or captured into the SIQD state i ($\tau_{cap,i}$). The QD capture process is mediated by Coulomb scattering and longitudinal optical phonon emission [3, 17]. Once captured into the SIQD state i, the electrons can either experience relaxation to a lower energy state ($\tau_{rel,QD,i}$) or recombine radiatively ($\tau_{rec,QD,i}$). Two mechanisms are reported to be responsible for the intraband relaxation of the electrons in the SIQD: Coulomb scattering is shown to be effective when the QW ground state is highly populated [3] whereas an Auger-like mechanism has been reported to mediate the relaxation in a low density case [18]. This Auger-like process involves the transition of an electron to a lower level in the SIQD, while a hole is ejected into one of the QW states. The QW-to-surface ($\tau_{W\to s}$) and QD-to-surface ($\tau_{D\to s}$) time constants describe the transition of carriers from the QW and QD to the surface, while τ_s represents the surface recombination time constant.

Based on the mechanisms described above, the rate equations for the carrier concentrations of QD level i ($N_{QD,i}$), the surface (N_s) and the QW (N_W) can be written as

$$\frac{dN_{QD,i}(t)}{dt} = -\frac{N_{QD,i}(t)}{\tau_{rec,QD,i}} + \frac{N_{QD,i+1}(t)}{\tau_{rel,QD,i+1}} f_i(t) - \frac{N_{QD,i}(t)}{\tau_{rel,QD,i}} f_{i-1}(t) + \frac{N_W(t)}{\tau_{cap}} f_i(t) - \frac{N_{QD,i}(t)}{\tau_{D,i\to s}} f_s(t), \quad (1)$$

$$\frac{dN_s(t)}{dt} = \frac{N_W(t)}{\tau_{W\to s}} f_s(t) + \sum_i \frac{N_{QD,i}(t)}{\tau_{D,i\to s}} f_s(t) - \frac{N_s(t)}{\tau_s}, \quad (2)$$

and

$$\frac{dN_W(t)}{dt} = -\frac{N_W(t)}{\tau_{rec,QW}} - \frac{N_W(t)}{\tau_{cap,i}} f_i(t) - \frac{N_W(t)}{\tau_{W\to s}} f_s(t), \quad (3)$$

where the state filling factor $f_x(t) = (D_x - N_x(t))$ is used because of the Pauli blocking, i.e., electrons can go only to an unoccupied state whereas the transition to an occupied state is prohibited. D_x is the density of states in level x (x is QD,i or s).

The following assumptions have been made in the calculations. (1) Recombination rate coefficients of all the QD states are assumed to be equal ($\tau_{rec,QD,i} \approx \tau_{rec,QD,}$). (2) Only the relaxation between the adjacent QD levels are taken into account and the coefficients of these transitions are assumed to be the same ($\tau_{rel,QD,i} \approx \tau_{rel,QD}$). (3) The probability of the electron capture from the QW to each QD level is equal ($\tau_{cap,i} \approx \tau_{cap}$). (4) The surface recombination rate is set to be linearly proportional to the electron density in the surface.

These assumptions are not correct at very high QW electron densities, since the rates are also proportional to the electron density in the initial state and to the density of available states in the final state [3]. As there is a considerable number of electron–hole pairs immediately after the excitation pulse, the first nanosecond has been omitted from the simulations in this work. Level populations for the initial state of the simulations were determined from the measurements at 1 ns. The rate equation analyses (ignoring the excitonic effects) are carried out by fitting the simulations to the experimental data.

4. Results and discussion

Figure 3 shows the time-resolved intensity of the QD0 PL peak from the sample with $d = 10$ nm. First, there is a slow decay component $\exp(-t/\tau_{dec,1})$ (dashed line, $\tau_{dec,1} = 3.2$ ns) which is followed by a faster component $\exp(-t/\tau_{dec,2})$ (dotted line, $\tau_{dec,2} = 1.5$ ns). Previously, the temporal behaviour of InGaAs/GaAs SIQDs has been shown to exhibit a two-component or biexponential decay [9], where an initial fast decay ($\tau_{dec,1} \sim 1$ ns) is followed by a slower decay ($\tau_{dec,2} \sim 4$ ns). The fast component was identified to originate from carriers that are captured directly into the QDs. A long-lived charge-separated state (CSS), on the other hand, was assigned to be responsible for the slow decay term. The CSS consists of an electron at the QW conduction band edge bound to a hole in the QD ground state [19]. Thus, the CSS was assumed to act as a reservoir which slowly feeds electrons into the QD. Moreover, an optical transition of the CSS was also observed (right below the QW energy) in the cw-PL spectra [9].

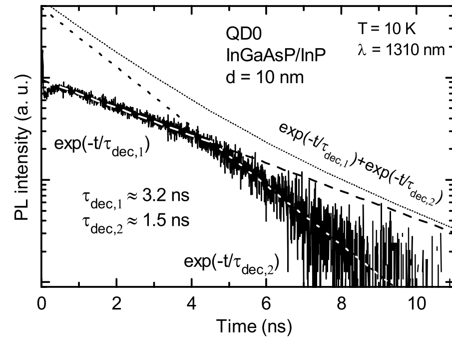

Figure 3. QD0 TRPL of an InGaAsP/InP sample with d =10 nm. Dashed and dotted lines are exponential fits. The sum of these terms is plotted with dots.

Table 1. Decay time constants of InGaAsP/InP QDs.

d (nm)	$\tau_{dec,1,QD0}$ (ns)	$\tau_{dec,2,QD0}$ (ns)	$\tau_{dec,2,QW}$ (ns)
7	1.4	0.8	0.2
10	3.2	1.5	0.3
13	3.4	1.6	0.4

There is evidently a fundamental difference between the InGaAs/GaAs and InGaAsP/InP SIQDs: for InGaAs/GaAs, the decay is biexponential, meaning that the fast and slow decay processes can coexist. As the fast component begins to die out, the slow component starts to dominate. However, as shown in figure 3, the temporal behaviour observed for the InGaAsP/InP QD is not biexponential but has a two-phase decay. This means that the temporal behaviour of the InGaAsP/InP QDs cannot be described with a sum of two exponential terms.

Figures 4(a) and (b) show the TRPL intensities corresponding to the QD0 and QW transients, respectively. The temporal behaviour of the QD0 transients show increasing slope as d is decreased from 13 to 7 nm. The same trend of decreasing decay time can also be observed in the behaviour of the QW transients. In table 1, decay time constants or effective carrier lifetimes are presented as determined by the exponential fits (as shown in figure 3 for $d = 10$ nm). For the QW transient only the faster decay time constant $\tau_{dec,2}$ could be determined.

In the latter part of the QD0 curves, carrier feeding from the higher energy level becomes more and more insignificant,

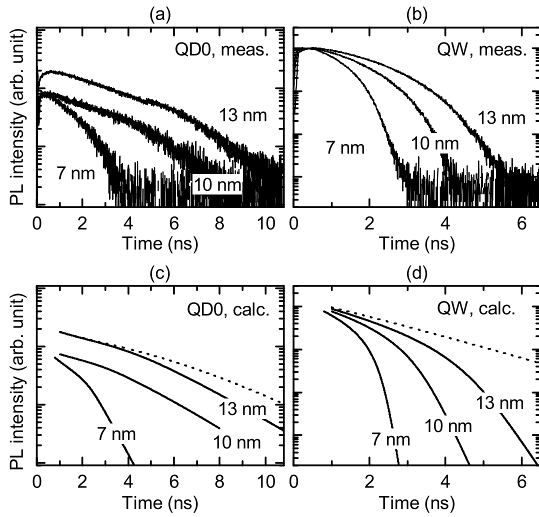

Figure 4. TRPL from InGaAsP/InP (a) QD0 and (b) QW with varying d. (c) and (d) show the calculated temporal behaviour according to the rate equation model for the QD0 and QW, respectively. For reference, the dotted lines are simulations with the rate equation model excluding the surface terms.

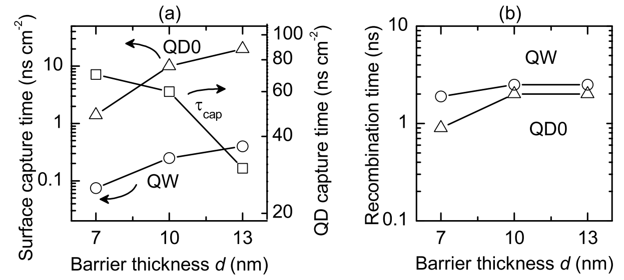

Figure 5. (a) Surface capture time constants for the QW and QD0 level and QD capture time constant (τ_{cap}) and (b) recombination time constants obtained for the QW and the QD0 level from the rate equation model.

meaning that the $\tau_{dec,2,QD0}$ is mostly determined by the radiative recombination and surface capture. Thus, the decay time constant $\tau_{dec,2,QD0}$ determined from the experimental PL curve, defines the lower limit for the time constant of the radiative recombination. In a way, the latter part of the time-resolved PL curve (with decreased number of carriers) can be also considered to represent a low-excitation case in cw-PL.

Relaxation of carriers from a higher energy state to a lower state (carrier feeding) plays an important role in this kind of multilevel energy structure. In an ideal case, the lower state would remain fully occupied until the higher state stops feeding carriers, i.e., becomes empty. Basically, the levels are emptied one by one, starting from the highest energy level. As reported for InGaAs/GaAs SIQDs, carrier feeding can cause somewhat similar plateau-like behaviour as seen in figure 4, and it cannot be excluded from the analysis [4]. However, carrier feeding alone does not explain the evident d-dependence seen in figure 4. Moreover, the fact that decreasing the barrier thickness d results in a shorter decay time for both the QD0 and QW levels indicates that the increased non-radiative recombination in the QW and QD is caused by surface related effects. It seems likely that carriers might be captured by the stressor islands on the surface due to the lower band gap of InAs. Carriers in the islands could then recombine radiatively or experience non-radiative recombination via surface states.

It has been reported that the surface depletion is suppressed and that surface band bending occurs in the region beneath InAs/InP and InAs/GaAs islands [20–22]. These effects have been assumed to be caused by the carrier accumulation in the InAs islands and by the surface states of the InAs islands. Same studies showed that an InAs wetting layer does not have such a significant effect. In this work, the QW TRPL transients of the reference samples with a surface wetting layer and samples without a surface wetting layer were virtually the same (not shown here). This also suggests that carriers captured away from the QW and QDs are mostly tunnelled into the InAs islands on the surface.

To extract more information on carrier dynamics, the TRPL measurements were analysed using the rate equation model including the surface terms described above. The simulations shown in figures 4(c) and (d) are in good agreement with the experimental data, showing the same trend of decreasing carrier lifetime with decreasing d. The dotted curves in (c) and (d) represent, for reference, the simulations performed with the rate equation model with the same parameters only excluding the surface terms. There is a clear difference between the models, which indicates that the surface states need to be included in the rate equation analysis.

Figure 5(a) shows the surface capture time and QD capture time constants obtained from the rate equation analyses. The probability of the carrier capture to the surface decreases by an order of magnitude as the barrier thickness d is increased from 7 to 13 nm. It should also be noted that the average time for an electron to experience surface capture from the QW is over ten times smaller as compared to the QD, i.e., the surface capture rate is larger for the QW. The recombination time constants of the QD0 and QW in figure 5(b), on other hand, do not show any significant dependence on the barrier thickness. The recombination time constant reported for InGaAs/GaAs SIQDs (0.86 ns [3]) is roughly the same as that determined for InGaAsP/InP SIQDs with $d = 7$ nm in this work (0.9 ns).

Figure 6(a) shows cw-PL spectra measured from InGaAsP/InP QDs with varying d. The dashed lines plot PL spectra measured with low excitation intensity, showing only the QD ground state and the QW peaks. The PL redshift (46–64 meV) of the QD0 transition from the QW peak, shown in (b), follows the depth of the confinement potential. Calculations have indicated that 80–90% of the redshift originates from the conduction band [11] (figure 1(d)). Thus, in the InGaAsP/InP QDs studied in this work, the QW ground state for an electron is ∼50 meV higher than the QD ground states. In other words, spatially under the stressor, an electron at the QW ground state experiences effectively an ∼50 meV smaller QW barrier to the surface. This difference in the barrier height provides a plausible explanation for the smaller surface capture time constants observed for the QW compared to that of the QD0 in figure 5(a).

In figure 6(a), not only does the QD0/QW PL intensity ratio diminish with decreasing d but also the absolute intensity of the QW PL peak increases. This results most likely from the

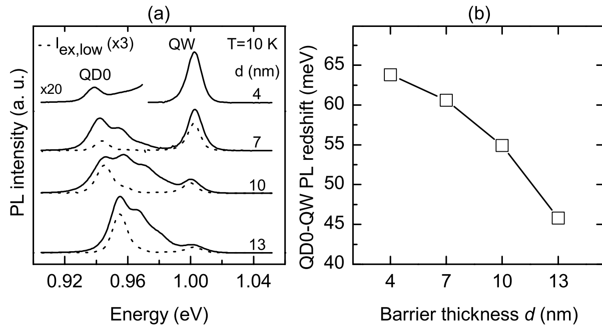

Figure 6. (a) PL spectra of InGaAsP/InP QDs with varying d. The PL spectra measured with low excitation intensity are plotted with dashed lines. The spectra are offset vertically for clarity. (b) The PL redshift of the QD0 from the QW as a function of barrier thickness d.

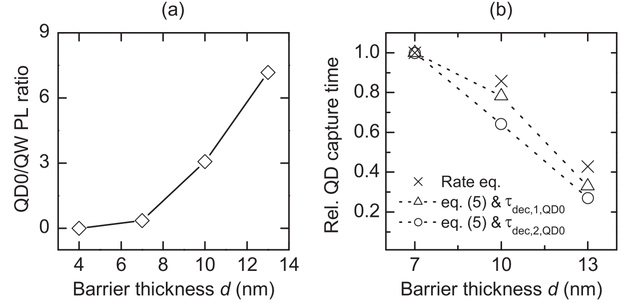

Figure 7. (a) The ratio of the integrated QD0 and QW PL intensities plotted as a function of the barrier thickness d and (b) comparison of QD capture time determined from the rate equation to calculated values from (5) using decay time constants from table 1. Crosses indicate capture times based on the rate equation model, whereas open triangles and circles correspond to calculations based on $\tau_{dec,1,QD0}$ and $\tau_{dec,2,QD0}$, respectively. QD capture time constants at $d = 7$ nm are normalized to 1.

reduced capture rate of carriers from the QW to the QD. The increasing surface capture (shown in figure 5(a)), on the other hand, is expected to be mainly responsible for the reduction of the integrated intensity of the PL spectra (by 60% between $d = 13$ and 4 nm). In general, it should be noted that a rather small variation of the barrier thickness d significantly affects the PL characteristics and that choosing d is a trade off between the achieved redshift and the surface capture time.

In the rate equation analyses, it was assumed that carriers first relax to the QW and then can experience radiative recombination, non-radiative recombination, or capture to the QD. Thus, the QW PL intensity is proportional to $\tau_{rec,QW}^{-1}/\tau_{dec,QW}^{-1}$, whereas the QD PL intensity is proportional to $\eta_{QD}\tau_{cap,QD}^{-1}/\tau_{dec,QW}^{-1}$. $\eta_{QD} = \tau_{rec,QD}^{-1}/\tau_{dec,QD}^{-1}$ is the quantum efficiency of the QD. Consequently, as pointed out by Lingk *et al* [9], in the low-excitation limit, where Pauli blocking effects can be neglected, the QD capture time constant τ_{cap} can also be determined from the equation

$$\eta_{QD}\tau_{cap}^{-1} = \frac{I_{QD}}{I_{QW}}\tau_{rec,QW}{}^{-1}, \tag{4}$$

where I_{QD}/I_{QW} is the ratio of the QD and QW photoluminescence intensities. Radiative recombination times of QW and QD ($\tau_{rec,QW}$ and $\tau_{rec,QD}$) were shown to be virtually independent of d (figure 5(b)). Thus, the d-dependent terms in (4) are effectively τ_{cap}, $\tau_{dec,QD}$, and the I_{QD}/I_{QW} ratio. Figure 7(a) shows the I_{QD}/I_{QW} ratio determined from the PL spectra in figure 6(a) by Gaussian fits to low-excitation PL peaks.

In order to compare the QD capture time constants obtained from the rate equation model (figure 5 (a)) to values calculated from (4), the values for $\tau_{rec,QW}$ and $\tau_{rec,QD}$ have been omitted, since they cannot be reliably established directly from the experimental results. They can only be determined by rate equation analysis. This is not expected to have a significant effect on the comparison of QD capture time constants with varying barrier thickness d, because $\tau_{rec,QW}$ and $\tau_{rec,QD}$ were found to be virtually independent of d. Hence, the QD capture time constants are calculated from equation

$$\tau_{cap}^{-1} \propto \frac{I_{QD}}{I_{QW}}\tau_{dec,QD}^{-1}. \tag{5}$$

The relative capture times presented in figure 7(b) have been normalized to 1 at $d = 7$ nm. Capture times calculated using $\tau_{dec,1,QD0}$ and $\tau_{dec,2,QD0}$ are plotted with open triangles and circles, respectively. The capture time from the rate equation model (crosses) seems to be in a rather good agreement with calculations based on (5). Thus, it seems that the rate equation model used in this work agrees with the experimental results.

The data presented in this paper do not give any evidence on whether the d-dependence of the QD capture is caused by the depth of the QD potential or by the height of the in-plane potential barriers around it (figure 1(d)). However, the characteristics of the CSS in InGaAs/GaAs SIQDs provide a possible answer [9]: since the time constant associated with the CSS showed very little dependence on d, it was concluded that the height of the in-plane barriers does not affect τ_{cap}. The modulated QW potential is basically the same in both systems. Therefore, one can assume that the depth of the QD potential is the decisive factor in determining the QD capture rate in InGaAsP/InP strain-induced QDs.

Although the tunnelling probability from the QD to the InAs islands on the surface is expected to be mostly determined by the barrier thickness d, the effect of the strain-induced QW barrier reduction is discussed. The strain ϵ is calculated by ΔT FEM method (as in figure 1). The effect of the strain on the band edge energy is, on the other hand, based on deformation potential theory [1, 23]: the strain components $\epsilon = \epsilon_{xx} + \epsilon_{yy} + \epsilon_{zz}$ and deformation potential constant a_c determine the change in the band edge energy $\Delta E_c = a_c\epsilon$ for the conduction band. The following (low-temperature) material parameters have been used for InP: $a_c = -6.0$ eV and $E_g = 1.42$ eV. For the $In_{0.56}Ga_{0.44}As$ QW (ΔE_C:ΔE_V = 0.43:0.57) the parameters were $a_c = -6.0$ eV and $E_g = 0.78$ eV (calculated using values of InAs and GaAs). The parameters are based on band parameters compiled by Vurgaftman *et al* [23].

The potential energy of the conduction and valence band edge under the stressor is plotted in figure 8 as a function of the distance from the surface. The conduction band edge energy of unstrained InP far from the surface is set to 0 eV. The incremental deformation in the valence band edge cannot be resolved in this scale. The conduction band, however, is pushed down more clearly with increasing strain. The effect

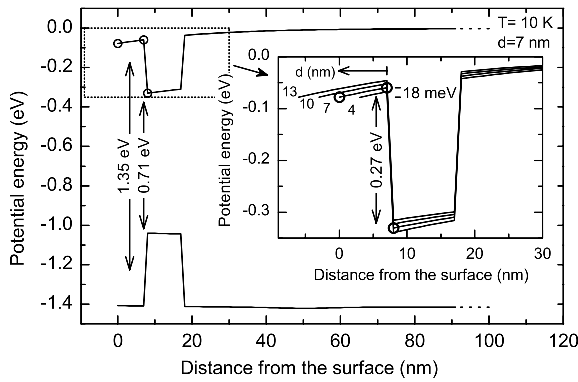

Figure 8. Calculated potential energy diagram of InGaAs/GaAs SIQD with $d = 7$ nm. The inset shows the conduction band potential energy of the QW and the top QW barrier with varying d. The circles are guides for the eye and the horizontal positions of the QWs in the inset are fixed for clarity.

can be seen distinctly in the inset, which shows the conduction band with varying barrier thickness d. As indicated, the barrier potential drops by 18 meV, which is ∼7% of the barrier height.

The effect of the strain-induced barrier reduction on the tunnelling probability of an electron was estimated by the basic quantum mechanic expression for the transmission probability for barrier penetration,

$$P_T = \exp\left(-2\sqrt{2m^*/\hbar^2}\int_0^d \sqrt{V(x) - E}\,\mathrm{d}x\right), \qquad (6)$$

where m^* is the effective mass of an electron (0.08 m_e) and $V(x)$ is the potential barrier. The tunnelled electron is assumed to be at the ground state energy E (6 meV above the conduction band minimum). For $d = 4$ nm the tunnelling probability P_T is 6% higher in the case of strain-induced potential barrier ($V(x)$ as shown in the inset of figure 8) than in the case of an ideal box potential ($V = 270$ meV). This indicates that the strain-induced QW barrier reduction might contribute to some extent to the surface capture probability, but the key factor is still the barrier thickness.

The results presented in this paper show that surface recombination plays an important role in the carrier dynamics of InGaAsP/InP SIQDs utilizing InAs stressor islands, and help in part to understand the fundamental physics involved in the QDs in general. On the whole, the findings indicate that the interplay between InAs nanostructures and two-dimensional electron gases needs to be taken into consideration while designing and fabricating low-dimensional device structures.

5. Summary

To conclude, the carrier dynamics in InGaAsP/InP quantum dots induced by self-assembled InAs stressor-islands was investigated. Time-resolved photoluminescence measurements along with cw-PL was used to study the effect of the distance d from the QW to surface on the characteristics of the QDs. The QDs were observed to exhibit a two-phase decay. The reduction of the carrier lifetime was caused by the recombination via stressor islands on the surface. However, a rather small increase of d was shown to enhance the QD luminescence significantly, due to decreased surface capture and partly due to increased QD capture rate. Moreover, detailed analysis using the rate equation model showed that the surface capture time constant can be increased considerably by controlling d.

Acknowledgment

The authors thank Professor Jukka Tulkki for his insight and help in the strain calculations.

References

[1] Tulkki J and Heinämäki A 1995 *Phys. Rev.* B **52** 8239
[2] Lipsanen H, Sopanen M and Ahopelto J 1995 *Phys. Rev.* B **51** 13868
[3] Brasken M, Lindberg M and Tulkki J 1997 *Phys. Status Solidi* a **164** 427
[4] Grosse S, Sandmann J H H, von Plessen G, Feldmann J, Lipsanen H, Sopanen M, Tulkki J and Ahopelto J 1997 *Phys. Rev.* B **55** 4473
[5] Sopanen M, Lipsanen H and Ahopelto J 1995 *Appl. Phys. Lett.* **66** 2364
[6] Pires M P, Landi S M, Tribuzy C V-B, Nunes L A, Marega E and Souza P L 2004 *J. Cryst. Growth* **272** 192
[7] Pagnossin I R, da Silva E C F, Quivy A A, Martini S and Sergio C S 2005 *J. Appl. Phys.* **97** 113709
[8] Lipsanen H, Sopanen M, Taskinen M, Tulkki J and Ahopelto J 1996 *Appl. Phys. Lett.* **68** 2216
[9] Lingk C *et al* 2000 *Phys. Rev.* B **62** 13588
[10] Wang T and Forchel A 1999 *J. Appl. Phys.* **86** 2001
[11] Riikonen J, Sormunen J, Koskenvaara H, Mattila M, Sopanen M and Lipsanen H 2005 *Japan. J. Appl. Phys.* **44** L976
[12] Sormunen J, Riikonen J, Mattila M, Sopanen M and Lipsanen H 2005 *Nanotechnology* **19** 1630
[13] Symonds C, Mangeney J, Saint-Girons G and Sagnes I 2005 *Appl. Phys. Lett.* **87** 012107
[14] Riikonen J, Sormunen J, Mattila M, Sopanen M and Lipsanen H 2005 *Japan. J. Appl. Phys.* **44** L518
[15] Taskinen M, Sopanen M, Lipsanen H, Tulkki J, Tuomi T and Ahopelto J 1997 *Surf. Sci.* **376** 60
[16] Koskenvaara H, Riikonen J, Sormunen J, Mattila M, Sopanen M and Lipsanen H 2006 *Physica* E at press
[17] Bockelmann U and Egele T 1992 *Phys. Rev.* B **46** 15574
[18] Brasken M, Lindberg M, Sopanen M, Lipsanen H and Tulkki J 1998 *Phys. Rev.* B **58** R15993
[19] Gu Y, Sturge M D, Kash K, Watkins N, Van der Gaag B P, Gozdz A S, Florez L T and Harbison J P 1997 *Appl. Phys. Lett.* **70** 1733
[20] Vicaro K O, Cotta M A, Gutirrez H R and Bortoleto J R R 2003 *Nanotechnology* **14** 509
[21] Tanaka I, Kamiya I, Sakaki H, Qureshi N, Allen S J Jr and Petroff P M 1999 *Appl. Phys. Lett.* **74** 844
[22] Takahashi T, Yoshita M, Kamiya I and Sakaki H 1998 *Appl. Phys.* A **66** S1055
[23] Vurgaftman I, Meyer J R and Ram-Mohan L R 2001 *J. Appl. Phys.* **89** 5815